POLITECNICO DI TORINO
Repository ISTITUZIONALE

GaN Devices for Motor Drive Applications

Original
GaN Devices for Motor Drive Applications / Palma, M., Musumeci, S., Mandrile, F., Barba, V.. - (2021), pp. 146-151. (8th Annual IEEE Workshop on Wide Bandgap Power Devices and Applications, WiPDA 2021 USA 2021) [10.1109/WiPDA49284.2021.9645113].

Availability:
This version is available at: 11583/2962063 since: 2022-04-26T13:33:40Z

Publisher:
Institute of Electrical and Electronics Engineers Inc.

Published
DOI:10.1109/WiPDA49284.2021.9645113

Terms of use:

This article is made available under terms and conditions as specified in the corresponding bibliographic description in the repository

Publisher copyright

(Article begins on next page)

19 November 2026

GaN Devices for Motor Drive Applications

Marco Palma
Director, Motor drives Systems and Applications
Efficient Power Conversion
Turin, Italy
marco.palma@epc-co.com

Salvatore Musumeci
DENERG - Politecnico di Torino
Corso duca degli Abruzzi 24, 10129
Turin, Italy
salvatore.musumeci@polito.it

Fabio Mandrile
DENERG - Politecnico di Torino
Corso duca degli Abruzzi 24, 10129
Turin, Italy
fabio.mandrile@polito.it

Vincenzo Barba
DENERG - Politecnico di Torino
Corso duca degli Abruzzi 24, 10123
Turin, Italy
vincenzo.barba@studenti.polito.it

***Abstract*—DC and battery-powered motor applications are shifting from conventional silicon MOSFET-based, low PWM frequency inverters to GaN-based, high-frequency PWM inverters. The advantages lie in the higher system efficiency and in the elimination of the electrolytic capacitors, and the DC input filter. In this paper, gallium nitride-based devices are shown to increase power density to a new level and move to high-frequency PWM inverters with negligible dead time for electric motors used in many different applications including, but not limited to: servo drives, e-bikes, e-scooters, collaborative and low-voltage robot, medical robots, industrial drones, and service-motors used in automobiles.**

Keywords— GaN inverter, motor drive, field-oriented control, reduced dead time, increased torque constant

I. Introduction

Today, many electrical motors require variable frequency drives to adapt the speed and the torque of the motor to the needs of the specific application operating point. Variable frequency drives are implemented with a two-level voltage source inverter topology, consisting of three phases because most motors are wound with three windings displaced by 120 electrical degrees. The permanent magnet motor, also known as DC brushless motor (BLDC), is widely used and offers higher torque capability per cubic inch and higher dynamics when compared to induction motors and to DC brushed motors. Permanent magnet motors require less current to generate torque because the flux is generated by the magnets in the rotor. The advent of the BLDC has been aided by motor control algorithms that allow a precise and controlled orientation of the magnetic field in the stator to get the optimum working point at every speed and at every torque. With these algorithms, the torque and phase current have a linear relationship [1].

Silicon-based power devices have been dominant in the inverter electronics, but today their performance is nearing their theoretical limits [2]. There is an increasing need for higher power density, in terms of amount of power, volume and weight the inverter can transfer to the motor from the DC source. Gallium nitride transistors and ICs have the best attributes to satisfy these needs. GaN devices have lower intrinsic carrier concentration, higher electric breakdown field, higher thermal conductivity, and larger saturated electron drift velocity when compared to silicon [3].

GaN's superior switching behavior helps to remove dead time and increase PWM frequency to obtain unmatched sinusoidal voltage and current waveforms for smoother, silent operation with higher system efficiency. Power density increases with the substitution of electrolytic capacitors in the input filter with smaller, cheaper, and more reliable ceramic capacitors.

The two-level, three-phases inverter topology is shown in Fig. 1. It consists of three switching legs that are connected to each motor phase and powered by a DC current source. In motor control applications, there is a controller circuit that consists of a digital processor that acquires phase currents and bus voltage data through analog-sensing circuits and implements the field-oriented control (FOC) motion algorithm.

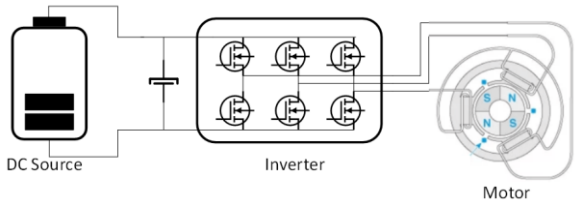


Fig. 1 DC Brushless motor system

In this article we will compare a generic inverter operated at 20 kHz with 500 ns dead time vs. a GaN inverter operated at 100 kHz with 14ns dead time in the same motor operating conditions. The 100 kHz GaN inverter shows higher total system efficiency and higher power density due to the removal of input electrolytic capacitors.

II. Power Dissipation in Motor and Inverter

A. Efficiency of different stages

The power dissipation and the subsequent overall efficiency in a DC inverter plus motor system depends on the efficiency of the inverter and motor stages in the specific operating point.

In Fig. 2, the inverter efficiency is calculated as $\eta_{inverter}=P_{out}/P_{in}$, while the efficiency of the motor is calculated

as $\eta_{motor} = P_{mech}/P_{out}$, and the overall efficiency is determined by the product of the two: $\eta = \eta_{inverter} \cdot \eta_{motor}$

where:

- P_{in} is the input power and is calculated as $P_{in}=V_{dcbus,rms} \cdot I_{dcbus,rms}$
- P_{out} is the output power; it is difficult to calculate it due to PWM modulation; it is usually measured with a three-phase power meter. For this paper, P_{out} is evaluated with a three-phase power meter specific software embedded in the Motor Drive Analyzer® Oscilloscope.
- P_{mech} is the mechanical power delivered to the load, calculated as $P_{mech}=T \cdot \omega$, where torque T and speed ω are measured by a torque/speed transducer.

As a result of the inverter control, the motor is generating a torque $T=k_t \cdot I_q$, where the I_q current is the controlled phase rms current when in field-oriented control operation, and k_t is the torque constant. When operated in field-oriented control, the inverter phase current I_{phase} is practically coincident with the I_q current. We will pose extreme attention to the I_{phase} harmonics, because, while all harmonics of I_{phase} contribute to the total I_{phase} rms current value, only the first harmonic contributes to the mechanical torque generation. Our aim is to reduce all higher order harmonics in the phase current, so that the motor effective torque constant k_t increases and approaches the ideal value in the ideal case of no power dissipation in the motor.

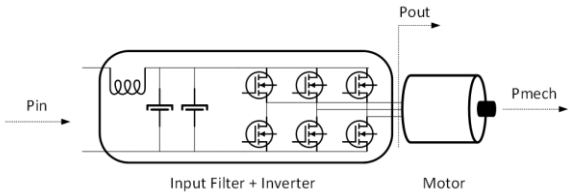


Fig. 2 Inverter stage and motor stage efficiency

B. Silicon inverter limitations

The inverter power dissipation is composed of conduction losses and switching losses. Conduction losses are directly proportional to the switches' channel resistance, $R_{DS(on)}$. Reducing the channel resistance helps to reduce conduction losses, but it can increase switching losses. The relation between conduction losses and switching losses depends on the specific switch technology.

DC and battery-operated motor drive applications have a DC bus voltage that spans from 24 VDC to 96 VDC. Typically, when silicon MOSFETs are used in the inverter, the PWM frequency is kept below 40 kHz, and the dead time is kept within the range of 200 ns to 500 ns. In this scenario, most of the power dissipation is due to conduction losses, since PWM frequency is kept low to avoid the switching loss penalty that becomes quite high with Si MOSFET technology.

Fig.3 shows an inverter integrated with the motor and connected to the battery with cables. During its switching operation, the low PWM frequency silicon inverter generates a ripple in the voltage and the current on the battery cables that become major sources of EMI. An LC filter is usually inserted between inverter and battery cables to reduce the interference. The LC filter dissipation enters in the efficiency equation, $\eta_{inverter}=P_{out}/P_{in}$, and reduces the inverter and the overall system efficiency.

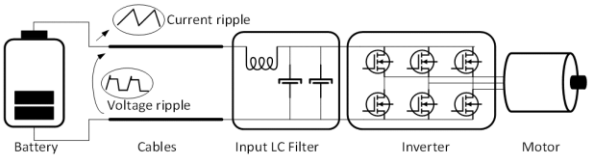


Fig. 3 Cables from the battery are the source of EMI and require the insertion of a LC filter at the inverter input

When dealing with silicon devices, the dead time is responsible for the 6th harmonic of the electrical frequency in the generated torque; this harmonic has no effect on the average torque applied to the load, it does not contribute to the motion, but does decrease the motor efficiency while increasing the vibrations transmitted to the load and the windings' temperature. When the 6th harmonic of the torque is present, the measured motor torque constant k_t is lower than the theoretical.

III. GaN Advantage

GaN devices, such as those from Efficient Power Conversion (EPC), show lower switching losses when compared to Si MOSFET and do not have a body diode *pn* junction, thus there is no associated reverse recovery in hard switching operation. These two factors combined help to eliminate the dead time and increase the PWM frequency to a point that the input filter made of one inductor and one or two electrolytic capacitors may be substituted with ceramic capacitors. The advantage is quieter operation with a smaller and lighter inverter. The motor runs smoother at a lower temperature and it is more efficient, since the 6th harmonic of the torque is completely removed. In addition, moving from electrolytic to ceramic capacitor reduces cost and increases system reliability.

A. GaN reverse capacitance C_{rss}

In the hard switching behavior analysis of a given device, it is essential to consider its reverse capacitance (C_{rss}) characteristics, its linearity, and the ratio between its low voltage value and its high voltage value ($C_{rsslow}/C_{rsshigh}$). In fact, C_{rss} plays a major role during the switching event, and the observed dv_{DS}/dt between drain and source is inversely proportional to C_{rss} and directly proportional to the I_{gate} current flowing in the gate during the Miller Plateau. Ideally, a C_{rss} that is constant versus voltage would simplify the gate driver design because the designer could just size the gate driving resistor to obtain the desired *dv/dt* slope. In actual conditions, C_{rss} value varies with applied drain-source voltage (V_{ds}) and, depending

on the technology used, the non-linearity affects the overall switching event.

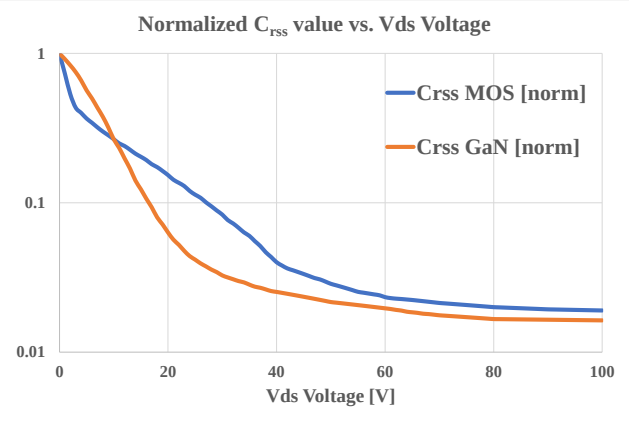


Fig. 4 Normalized C_{rss} vs. Vds Voltage [V] of BSC027N10NS5 (MOS) and EPC2022 (GaN)

Conventional gate driving is done by applying a voltage to the gate of the switch through a resistor. If the value of the ratio $C_{rsslow}/C_{rsshigh}$ is too high, either of the following conditions can occur:

- the switch is too fast at the beginning of the turn-on event, leading to high *dv/dt*
- the switch is too slow at the end of the turn-on event, leading to a tail effect and higher power dissipation

In Fig. 4, the normalized curves of C_{rss} versus voltage of a 100 V MOSFET and a 100 V eGaN® FET from EPC are shown. The commutation waveforms of the eGaN device are smoother because the C_{rss} curve is more linear than the MOSFET.

B. Absence of intrinsic body diode

In a MOSFET there is an intrinsic *pn* body diode that has an important effect in the hard commutation of a half-bridge leg. When a MOSFET in a half bridge is turning on against the body diode of its complementary switch, it must deal with the reverse recovery current, that depends on load current and on the turn on *di/dt* [5]. In MOSFET based motor drives, it is common practice to slow down the turn-on event to reduce *di/dt* and to reduce the reverse recovery current; however, this requires an increase to the minimum dead time that can be applied to the half bridge.

In a GaN FET, the absence of an intrinsic body diode, and its associated reverse recovery, allows having a repeatable and smooth *dv/dt* that, in turn, allows a reduction of the dead time.

C. Dead time elimination and its effect

In standard inverters for motor drive applications, the dead time between the complementary switches of a half-bridge leg is essential to avoid shoot through events. Usually, a value between 200 ns and 1 µs is used, with the effect of introducing non-linearities and discontinuities in the applied voltage waveform to three-phase load.

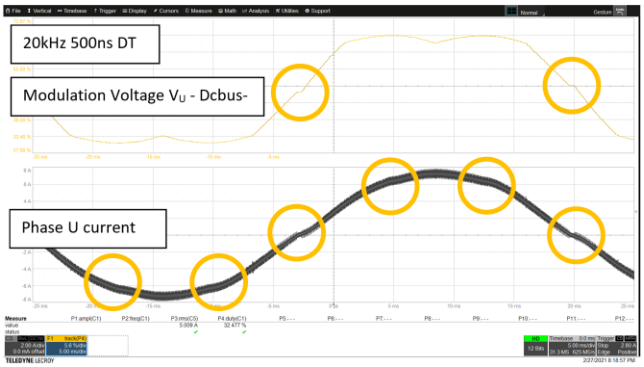


Fig. 5 Voltage modulation and phase current at 20 kHz with 500ns dead time

Several attempts to mitigate the effect of the dead time have been investigated ([5] and [6]).

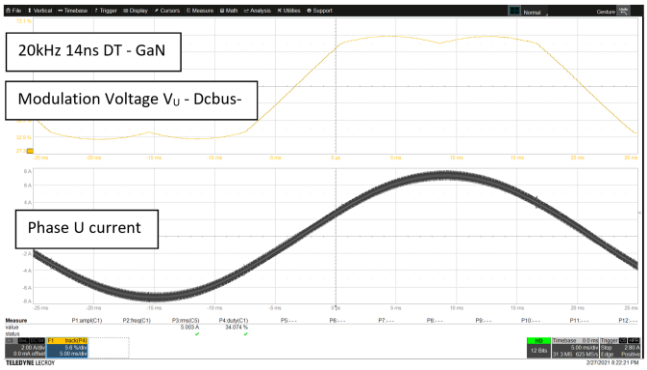


Fig. 6 Voltage modulation and phase current at 20 kHz with 14ns dead time

In [7] an inverter with 500 ns dead time has been compared to an inverter with 500 ns dead time and software compensation of the dead-time effect, and to a GaN inverter with negligible dead time (14 ns) and no software compensation. The clear advantage of a GaN inverter is that it allows reducing to tens of nanoseconds the dead time without requiring any effort in the computation from the digital controller (no software compensation is needed). Fig. 5 and 6 show the difference in modulation voltage and phase current between two different dead-time values. Eliminating the dead time improves the quality (in terms of THD) of the applied sinusoidal voltage that is, in turn, reflected in less distortion in the phase current, less vibrations, and less acoustic noise generated by the motor.

Analyzing in the *dq* reference frame, the effect of the dead time shows up as a balanced waveform over-imposed to the I_q current, with six period per each electrical cycle [7]. Fig. 7 shows the behavior of the ripples imposed to the I_d and I_q currents, when operating in field-oriented control and the phase current has unitary amplitude.

When observing the I_{phase} current digital Fourier transform (DFT), the discontinuities due to the dead time appear as a 5^{th} and a 7^{th} harmonic of the phase current [7]. These harmonics are convoluted to a 6^{th} harmonic of the torque applied to the motor as it can depicted in Fig. 8. The torque DFT signals shown in Fig. 8 and in Fig. 9 have been measured

experimentally by using an analog torque/speed transducer physically connected between the motor and the load in the

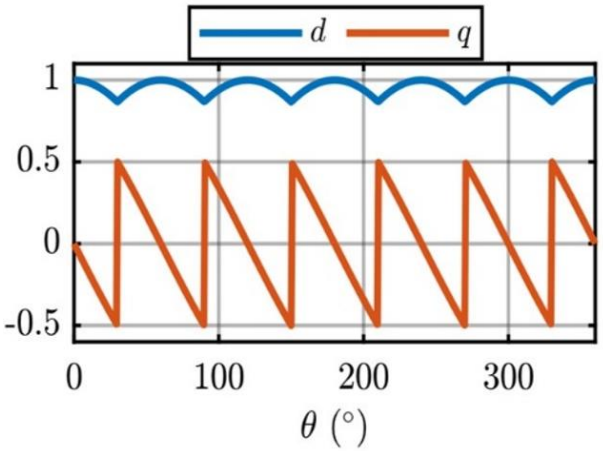


Fig. 7 *sign*(I_{phase}) function in per unit in the rotating (*d*,*q*) frame, synchronous with the phase current I_{phase}.

motor bench setup shown in Fig. 12. The DFT has been calculated by the oscilloscope specific function.

Fig. 9 shows the effect of the dead-time elimination when using GaN inverter: the 6th harmonic of torque disappeared, while the rms value of the phase current is kept the same. This means that the DC component of the torque in the second case has increased.

D. PWM frequency increase effect

A GaN inverter can easily be operated at 100 kHz PWM frequency, thanks to its lower switching dissipation and smoother switching at the allowed *dv/dt*. Considering the worst case of a pure inductive load and using a first order approximation (1) of the equations, the input voltage ripple is inversely proportional to the PWM switching frequency f_{PWM}, the input capacitance value C_f, and directly proportional to the inverter output peak current I_0 [8].

$$\Delta v_{pp} \propto \frac{1}{4 f_{PWM}} \frac{I_0}{C_f} \tag{1}$$

If the PWM frequency is increased from 20 kHz to 100 kHz, the input capacitance can be reduced by at least a factor of five to preserve the same input voltage ripple. Capacitor technology plays a crucial role, in the sizing of the inverter system. Thus, by increasing the PWM frequency the reduction factor is bigger than the theoretical.

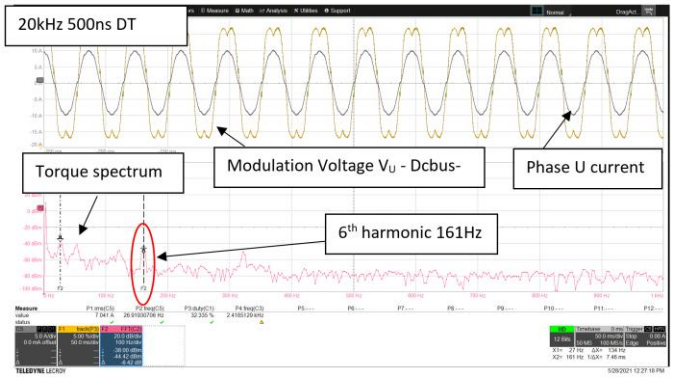


Fig. 8 500ns dead time effect on torque signal; electrical frequency is 27 Hz, 6th harmonic is visible.

The input current ripple is also inversely proportional to the PWM frequency. During a PWM cycle each half bridge leg of the inverter can be considered equivalent to a buck converter at constant current and similar formulas (2) apply.

$$\Delta I_D \cong \frac{\Delta V \cdot D}{f_{PWM} \cdot L} \tag{2}$$

Increasing the PWM frequency has then the double effect of reducing both the input current ripple and the input voltage ripple.

With low PWM frequencies (20 kHz), the required input capacitance requires the designer to use polarized capacitors; electrolytic or tantalum. The electrolytic capacitors pose limits on the amount of the RMS current they can support, and it is common to use a capacitance value that is quite bigger than the theoretically minimum needed. When the PWM frequency is increased, the minimum required capacitance decreases allowing the use of ceramic capacitors. This brings several advantages to the design because ceramic capacitors exhibit lower series impedance with a minimum in the region between 100 kHz and 200 kHz, are more stable in temperature, and are more reliable [9].

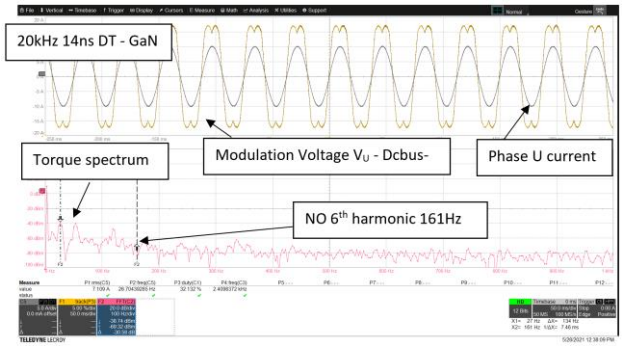


Fig. 9 GaN inverter with 14ns dead time and its effect on torque signal; electrical frequency is 27 Hz, torque 6th harmonic is null

The high frequency operation enabled by GaN devices also benefits the electric machine, from the point of view of the additional PWM-induced losses [10], being the current ripple of smaller magnitude.

Fig. 10 and 11 show the input current ripple, the input voltage ripple, and the output current ripple when comparing two different setups consisting of:

- conventional inverter with LC input filter (Fig. 3) at PWM = 20 kHz, dead time = 500 ns, L = 6 µH, and C = 2 x 330 µF.
- GaN inverter without input filter at PWM = 100 kHz, dead time = 14 ns, and C = 2 x 22 µF.

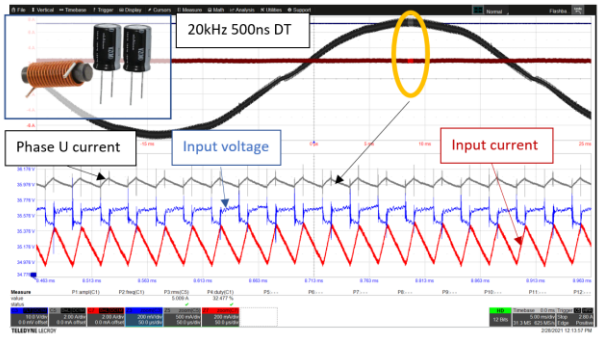


Fig. 10 Conventional inverter with LC input filter at PWM = 20 kHz, dead time = 500 ns, L = 6 µH, and C = 2 x 330 µF eCaps; Phase U current 500 mA/div, Input voltage 200 mV/div, input current 200 mA/div, and 50 µs/div zoom timescale

Both the conventional inverter with LC input filter and the GaN inverter without an input filter are running an e-bike motor at 36 V_{DC} battery voltage and 5 A_{RMS} phase current. The input voltage and current ripples are similar, so, even if the solution at 100 kHz does not have an input filter, the same conducted EMI as in first solution with filter at 20 kHz is expected. In the second solution, the output current ripple is reduced and the current in the motor has a better sinusoidal shape.

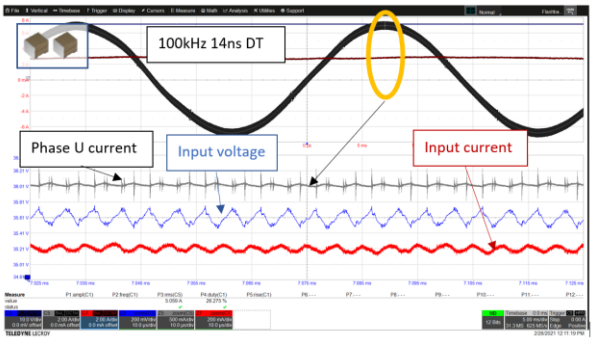


Fig. 11 GaN inverter without input filter at PWM = 100 kHz, dead time = 14 ns, and C = 2 x 22 µF ceramic; Phase U current 500 mA/div, Input voltage 200 mV/div, input current 200 mA/div and 10 µs/div zoom timescale

E. System efficiency

When comparing the two setups used in Fig. 10 and 11 using a power meter system, the GaN inverter running at 100 kHz PWM and 14 ns dead time shows higher system efficiency than the conventional inverter running at 20 kHz frequency, 500 ns, and with an input LC filter. Table 1 shows that by moving from a silicon-based 20kHz inverter to a GaN-based 100 kHz inverter with almost no dead time, the input filter is reduced in size, weight and cost, and the total system efficiency in the specific operating point is increased by 6.5 points.

TABLE 1 EXPERIMENTAL RESULTS

Setup	**Inverter** **20kHz 500ns dead time** **400 RPM 5 Arms**	**GaN inverter** **100kHz 14ns dead time** **400 RPM 5 Arms**
Input Inductance	2.7 µH	None
Input capacitor	660 µF electrolytic	44 µF ceramic
Input power to the inverter	121.3 W	113.3 W
Output power from the inverter	119.6 W	111.3 W
$\eta_{inverter}$	98.5 %	98.2%
Motor speed	42.25 rad/s	41.94 rad/s
Torque	1.876 N	1.940 N
Mechanical Power	79.3 W	81.36 W
η_{motor}	66.3 %	73.1 %
η total efficiency	65.3 %	71.8 %

F. Hardware Setup

Hardware setup is shown in Fig. 12.

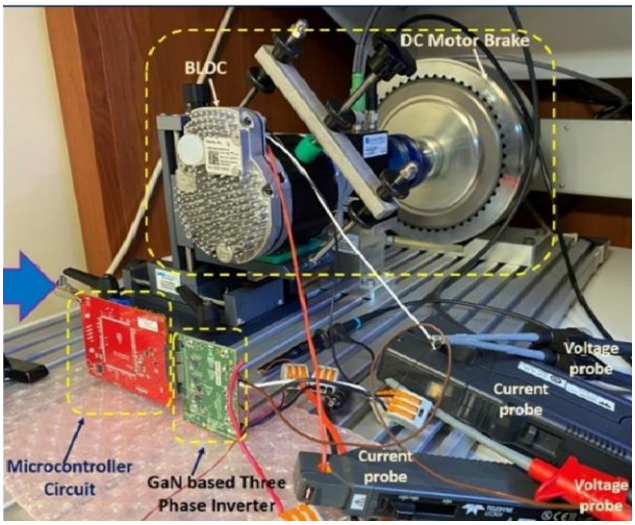


Fig. 12 Hardware setup. Between motor and Brake there is a torque/speed transducer

IV. Conclusions

DC and battery powered motor applications are moving from conventional Si MOSFETs and low PWM frequency inverters to GaN-based, high frequency PWM inverters. The increase of the PWM frequency allows the reduction of the input filter, while the elimination of the dead time allows getting a higher k_t torque constant from the motor, thus improving the overall efficiency. The advantages are a higher system efficiency and the elimination of the electrolytic capacitors and input inductor.

References

[1] Amin, Faisal & Sulaiman, Erwan & Soomro, Hassan. (2019). Field Oriented Control Principles for Synchronous Motor. International Journal of Mechanical Engineering and Robotics Research. 8. 284-288. 10.18178/ijmerr.8.2.284-288.

[2] Baliga, B. J., "Power semiconductor device figure of merit for high frequency applications," IEEE electron Device Lett., vol. 10, p. 455, Oct. 1989.

[3] Lidow, A., de Rooij, M., Strydom, J., Reusch, D., Glaser, J., GaN Transistors for Efficient Power Conversion, 3rd ed., Wiley, 2020, pp. 1-6.

[4] Glaser, J., Reusch, D., "Comparison of deadtime effects on the performance of DC-DC converters with GaN FETs and silicon MOSFETs," 2016 IEEE Energy Conversion Congress and Exposition (ECCE)

[5] Zhengyi, he & Ji, Xuewu. (2008). A new inverter compensation strategy based on adjusting dead-time on-line. IEEE International Symposium on Industrial Electronics. 10.1109/ISIE.2008.4676957.

[6] Lee, Joon-Hee & AE, Seung-Ki. (2021). Inverter Nonlinearity Compensation through Dead Time Effect Estimation. IEEE Transactions on Power Electronics. PP. 1-1. 10.1109/TPEL.2021.3061285.

[7] Mandrile, F.; Musumeci, S.; Palma, M. Dead Time Management in GaN Based Three-Phase Motor Drives. Proceeding of the 23rd European Conference on Power Electronics and Applications, EPE'21 ECCE Europe. 6–10 September 2021, Virtual Conference, pp 1-10.

[8] Vujacic, M., Hammami, M., Srndovic, M., Grandi, G., "Analysis of dc-Link Voltage Switching Ripple in Three-Phase PWM Inverters," Energies. 2018; 11(2):471. https://doi.org/10.3390/en11020471.

[9] Gurav, Abhijit & Bultitude, John & McConnell, John & Phillips, Reggie. (2018). Robust Reliability of Ceramic Capacitors for Power Electronics. Additional Conferences (Device Packaging, HiTEC, HiTEN, & CICMT). 2018. 000138-000142. 10.4071/2380-4491-2018-HiTEN-000138.

[10] D. Cittanti, V. Mallemaci, F. Mandrile, S. Rubino, R. Bojoi, and A. Boglietti, "PWM-Induced Losses in Electrical Machines: An Impedance-Based Estimation Method," 2021 24rd International Conference on Electrical Machines and Systems (ICEMS), 2021, in press.